JOURNAL OF GUIDANCE, CONTROL, AND DYNAMICS
Vol. 19, No. 5, September–October 1996

Closed-Loop, Estimator-Based Model of Human Posture Following Reduced Gravity Exposure

Dava J. Newman,* Karl U. Schultz,† and Jennifer L. Rochlis‡
Massachusetts Institute of Technology, Cambridge, Massachusetts 02139

A computational and experimental method is employed to provide an understanding of a critical human space flight problem, posture control following reduced gravity exposure. In the case of an emergency egress, astronauts' postural stability could be life saving. It is hypothesized that muscular gains are lowered during reduced gravity exposure, causing a feeling of heavy legs, or a perceived feeling of muscular weakness, upon return to Earth's 1 *g* environment. We developed an estimator-based model that is verified by replicating spatial and temporal characteristics of human posture and incorporates an inverted pendulum plant in series with a Hill-type muscle model, two feedback pathways, a central nervous system estimator, and variable gains. Results obtained by lowering the variable muscle gain in the model support the hypothesis. Experimentally, subjects were exposed to partial gravity ($\frac{3}{8}$ *g*) simulation on a suspension apparatus, then performed exercises postulated to expedite recovery and alleviate the heavy legs phenomenon. Results show that the rms position of the center of pressure increases significantly after reduced gravity exposure. Closed-loop system behavior is revealed, and posture is divided into a short-term period that exhibits higher stochastic activity and persistent trends and a long-term period that shows relatively low stochastic activity and antipersistent trends.

Nomenclature

A	= state space equation matrix
B	= Hill muscle model dashpot parameter
$\boldsymbol{B}$	= state space equation matrix
$\boldsymbol{C}$	= state space equation matrix
D	= diffusion coefficient
$\boldsymbol{D}$	= state space equation matrix
G	= variable muscle gain
g	= acceleration due to gravity ($1\ g = 9.8$ m/s^2)
H	= correlation coefficient
I	= moment of inertia
$\boldsymbol{I}$	= 2×2 identity matrix
K	= Hill muscle model spring parameter
$\boldsymbol{K}$	= optimal feedback gain matrix
$\boldsymbol{L}$	= optimal estimator gain matrix
l	= leg length
m	= body mass
N	= noise matrix
$\langle r^2 \rangle$	= average squared distance between center of pressure points
s	= Laplace transform
T	= applied tension
T_0	= force generator tension
u	= control input torque
x	= state of the plant
$\boldsymbol{x}$	= anteroposterior (front-to-back) axis
y	= output of the plant
$\boldsymbol{y}$	= mediolateral (side-to-side) axis
Δt	= time interval
$\langle \Delta x^2 \rangle$	= mean square displacement
θ	= inverted pendulum ankle angle
τ	= ankle torque

Subscripts

cog	= cognitive variable
ip	= inverted pendulum plant state space matrices
l	= one-half of the long time constant slope
m	= muscle plant state space matrices
PE	= parallel elastic component
p	= plant state space matrices
r	= reflexive feedback state space matrices
SE	= series elastic component
s	= one-half of the short time constant slope
v	= vestibular/visual feedback state space matrices
$\boldsymbol{x}$	= anteroposterior axis
$\boldsymbol{y}$	= mediolateral axis

Superscripts

$\dot{}$	= derivative with respect to time
$\ddot{}$	= second derivative with respect to time
$\hat{}$	= estimated state of the system

Introduction

A GOAL of this paper is to apply control methodology to a topic related to human space flight and to introduce the journal's audience to these new developments. The ability for astronauts to stand upright upon returning to Earth's 1 *g* (9.8 m/s^2) or other planetary environment after space flight is essential. An astronaut's stable posture control during an emergency egress could be life saving. To familiarize the reader with concepts important to this research effort, a few engineering analogues are given for the neuromuscular system. Working muscles are controlled by nerves and their wiring diagrams link muscles, reflexes, and muscle proprioceptors (specialized sensory receptors in the body responsible for motor functions) that are critical in posture control. Motor pathways arise in the central nervous system (CNS), or controller, and electrical signals descend to the skeletal muscles, or actuators. Within muscles are stretch receptors that experience the same relative length change as the overall muscle, akin to a position transducer. Other proprioceptors found in tendons, close to the muscle, act as force transducers because they are in series with muscles and increase the frequency of electrical activity in response to tendon stretch that accompanies an increase in muscle tension. The increased firing rate controls the level of force in the muscle and signals are transmitted back to the CNS, thus closing the loop from CNS to muscles and back. There is also evidence that muscle stiffness is the controlled quantity rather than length or force discretely,[1] and impedence characteristics of motor control are actively being studied.[2–5]

Received Oct. 17, 1995; revision received May 7, 1996; accepted for publication May 13, 1996.

*Assistant Professor, Department of Aeronautics and Astronautics, Room 33-119, 77 Massachusetts Avenue. Member AIAA.

†Graduate Fellow, Department of Aeronautics and Astronautics; currently Lt. J.G., U.S. Navy.

‡Research Assistant, Department of Aeronautics and Astronautics.

There have been many attempts to apply control theory to the analysis of human movement,[6–9] but the neuromuscular mechanics underlying human posture control following reduced gravity exposure involve a complex and not fully understood sensorimotor control system. An analogy of controlling an unstable, inverted pendulum by maintaining the center of pressure (COP) within the bounds of stability (projection of the feet) at all times is suggested. The COP, positioned directly below the center of mass of the subject, is the point at which the resultant force exerted on the ground by the subject is located. If the COP travels beyond the bounds of stability and the subject is not able to produce ankle torque to counter the direction of motion without moving his/her feet, the subject will be unstable and will fall.

Our estimator-based control model provides a computational method to investigate the hypothesis that a heavy legs phenomenon, or a perceived feeling of muscular weakness upon return to 1 g, is a result of lowered muscular gains during reduced gravity exposure. Experimental posture control studies in 1 g have concluded that deteriorated postural stability is linked to excitation of sensory receptors in the lower legs.[10] The model input is ankle torque, and the output is controlled ankle angle required for stability. The model incorporates an inverted pendulum placed in series with a Hill-type muscle model[11] that incorporates both active and passive muscle characteristics by including a parallel elastic component K_{PE} in parallel with a contractile component (a force generator in parallel with a nonlinear dashpot), and these components are placed in series with a series elastic component K_{SE}. Where the series elastic and parallel elastic components account for passive muscle characteristics, the contractile component accounts for active muscle characteristics. The combination of the muscle model and the inverted pendulum model creates the plant. Two feedback paths, a reflexive path that uses the system states for feedback and a vestibular/visual feedback path that uses the states of the system reconstructed by a CNS estimator, are included in the model. The CNS internal estimator makes the model more realistic since in determining the position of the body and the appropriate stabilizing response, the CNS integrates signals from various sources. Simply feeding the state values to the CNS would be inadequate. A variable gain preceding the plant represents the activation level of the leg muscles, and by manipulating this parameter the heavy legs phenomenon is illustrated.

Posture tests have shown that humans use a variety of sensory inputs in a feedback manner to maintain upright posture. Visual, vestibular, and proprioceptive cues are all used, although Dietz and Horstmann[12] reported that the removal of the visual cue did not significantly change subject performance, in contrast to the findings of Paulus et al.,[13] Ring et al.,[14] and Collins and De Luca.[15] Upon return from space, investigators found an increased reliance on visual cues in subjects in addition to the appearance of some postural instabilities because of either orthostatic intolerance (faintness and an inability to stand upright as a result of a lack of blood flow against gravity) or vestibular conflict upon return to a 1 g environment.[16] The vestibular system contains the body's internal navigation system, namely, linear and angular acceleration sensors for orientation. Kenyon and Young[17] found decrements in standing ability with the eyes closed for several days following space flight, and subjects only maintained upright posture if they stayed within a very narrow cone of static stabilty near the vertical. In posture platform tests, astronauts demonstrated abnormal postural sway oscillations and drift immediately postflight when the support was sway-referenced to eliminate ankle proprioception cues.[18] Reflex motions, upright posture, and locomotion all depend on receptors in and around joints, primarily located in the ligaments that stabilize the joint (Ref. 8, p. 144), that respond to joint angle.

The aim of the experimental study described herein was to determine the effects of acute partial gravity exposure on subjects' standing ability and, specifically, to provide necessary data to confirm or to reject the hypothesis that muscular gains are lowered during reduced gravity exposure causing a heavy legs phenomenon upon readapting to 1 g. In addition, one of three exercise protocols was given to subjects after partial gravity exposure to investigate neuromuscular adaptation and recovery. Posture control is often assessed experimentally by instrumenting a force platform and measuring maximum displacement, mean squared displacement, and total distance traversed by the COP under a subject's feet. Collins and De Luca[15,19] have successfully used stabilogram-diffusion analysis to reveal COP trajectories and to suggest neuromuscular mechanisms involved in maintenance of upright posture. Using stabilogram-diffusion analysis, namely, spatial and temporal analysis of COP trajectories, one can objectively evaluate changes in sway stability strategies and performance and can compare those changes between gravity conditions and among subjects. Spatial analysis includes computation of the root mean square (rms) position of the COP in the x and y axes, as well as the planar rms. It is hypothesized that the rms of the COP will increase following brief exposure to reduced gravity locomotion being less stable as a result of adaptively reweighted (reduced) muscular gain inputs. Temporal analysis reveals the position and change in COP position as a function of time, allowing stochastic activity with self-correlation factors to be determined. Stabilogram-diffusion analysis is used to examine the quiet standing posture data and has shown that postural response can be broken into two separate regions: the short-term region is characterized by a high level of stochastic activity and persistent behavior that is driven by the inertial characteristics of the system, and the long-term region exhibits a lower level of stochastic activity and antipersistent behavior because of the closed-loop nature of the system.[19] No change is expected in the temporal characteristics of posture following acute low-gravity exposure.

Method

Estimator-Based Model

As mentioned previously, a human standing erect can be modeled as a rigid inverted pendulum with length l equal to a leg length of 1 m and the total body mass of a typical subject ($m = 77$ kg) concentrated at the hips. For this model, the pendulum (angular acceleration) is controlled by two torques applied at the ankles, one in each axis. The three-dimensional model can be simplified into two uncoupled, linear models, each with the following governing equation (similarly for the y axis):

$$\ddot{\theta}_x = \frac{-mg\sin\theta_x}{I} + \frac{\tau_x}{I} \tag{1}$$

The moment of inertia for a point mass at the end of a rigid bar is ml^2.

The entire system can be linearized and modeled using the following state space equations:

$$\dot{x} = \boldsymbol{A}x + \boldsymbol{B}u \tag{2}$$

$$y = \boldsymbol{C}x + \boldsymbol{D}u \tag{3}$$

where

$$x = \begin{bmatrix} \dot{\theta}_x \\ \theta_x \\ \dot{\theta}_y \\ \theta_y \end{bmatrix} \qquad y = \begin{bmatrix} \theta_x \\ \theta_y \end{bmatrix} \qquad u = [\tau_x \quad \tau_y]$$

The inverted pendulum matrices are defined as

$$\boldsymbol{A}_{\mathrm{ip}} = \begin{bmatrix} 0 & g/l & 0 & 0 \\ 1 & 0 & 0 & 0 \\ 0 & 0 & 0 & g/l \\ 0 & 0 & 1 & 0 \end{bmatrix} \qquad \boldsymbol{B}_{\mathrm{ip}} = \begin{bmatrix} -1/ml^2 & 0 \\ 0 & 0 \\ 0 & -1/ml^2 \\ 0 & 0 \end{bmatrix}$$

$$\boldsymbol{C}_{\mathrm{ip}} = \begin{bmatrix} 0 & 1 & 0 & 0 \\ 0 & 0 & 0 & 1 \end{bmatrix} \qquad \boldsymbol{D}_{\mathrm{ip}} = \begin{bmatrix} 0 & 0 \\ 0 & 0 \end{bmatrix}$$

To account for the characteristics of the muscular actuators in this system, the Hill muscle model is placed in series with the pendulum model. Assuming that there is no muscular length change during quiet standing, the relationship between the force generator tension or desired tension T_0 and the applied tension T can be described as

$$T = \left(\frac{K_{SE}}{Bs + K_{PE} + K_{SE}}\right) T_0 \tag{4}$$

This relationship can be converted into single-input/single-output (SISO) state space format by creating an intermediate plant state x. The state space matrices for the muscle plant in x and y axes are

$$\begin{aligned} \boldsymbol{A}_m &= \frac{-(K_{PE} + K_{SE})}{B}\boldsymbol{I}, \qquad & \boldsymbol{B}_m &= \boldsymbol{I} \\ \boldsymbol{C}_m &= \frac{-K_{SE}}{B}\boldsymbol{I}, \qquad & \boldsymbol{D}_m &= 0 \end{aligned} \tag{5}$$

The constants in this model are assigned as

$$B = 41{,}710 \text{ Ns/m}$$

$$K_{PE} = 200 \text{ N/m}$$

$$K_{SE} = 97{,}190 \text{ N/m}$$

These numbers can vary greatly depending upon subject, muscle type, muscle size, and muscle activation level, but represent realistic values for a young adult with an activated muscle.[20] Figure 1a shows an initial block diagram with control torque u as the input to the muscle plant characterized by the muscular force generator, dashpot, parallel elastic, and series components used for posture control, and the inverted pendulum plant representing human standing with ankle angular displacement (body angle) ouput. Figure 1b shows the combined plant block diagram.

Although the plant is inherently unstable, through reflexive feedback, the system can be stabilized. In this model the muscle stretch reflex is the primary engine for reflexive stability. By responding to changes in body angles and time rates of change in angles, the stretch reflex keeps the modeled person standing upright. This mode of stability is crude and results in a swift jerky motion but succeeds in stabilizing the system. The stretch reflex is modeled as a full state feedback loop with an optimal feedback gain $\boldsymbol{K}_r$. A pure time delay (30 ms) is then placed in the feedback loop to model the delays in the monosynaptic stretch reflex. The delay is actually modeled as the Pade approximation of a pure time delay, which uses a nonminimum phase zero (zero in the right half-plane) and a stable pole to create additional lag without changing the gain of the system. With a time delay of τ, the SISO reflexive state space equations become

$$\begin{aligned} \boldsymbol{A}_r &= (-2/\tau)\boldsymbol{I}, \qquad & \boldsymbol{B}_r &= \boldsymbol{I} \\ \boldsymbol{C}_r &= (4/\tau)\boldsymbol{I}, \qquad & \boldsymbol{D}_r &= -\boldsymbol{I} \end{aligned} \tag{6}$$

Noise was added before the time delay to account for uncertainties in the states of the system. A noise value of $N_r = 0.008$ represents a random, zero mean, normally distributed error with a variance of approximately 1 deg in the estimated states of the system.

Of course, reflex is not the only stabilizing feedback involved in posture control. The CNS integrates signals from various sources to determine the position of the body and the appropriate stabilizing response. However, instead of simply feeding the state values to the CNS, the model is made more realistic by assuming that the

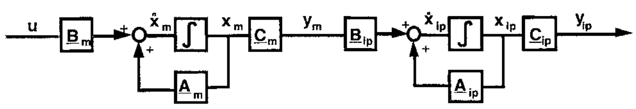

Fig. 1a Block diagram depicting model plants.

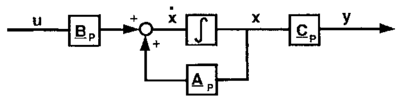

Fig. 1b Overall model plant block diagram with input torque and output displacement.

CNS cannot instantly determine the angle that the body makes with the vertical. Instead, posture control is accomplished by estimating body angles through an internal representation of the plant through the estimator state space equations for high-level CNS control but not subcortical functions such as the stretch reflex. The equations for the CNS estimator are

$$\dot{\hat{x}} = \boldsymbol{A}_p\hat{x} + \boldsymbol{B}_p u - \boldsymbol{L}(y - \hat{y}) \tag{7}$$

$$\hat{y} = \boldsymbol{C}_p\hat{x} + \boldsymbol{D}_p u \tag{8}$$

where $\boldsymbol{L}$ is found using the algebraic Riccati equation. The CNS then compares its estimate of the output $\hat{y}$ to the plant output y.

The assumption is made that the CNS, using its estimates of the states of the system, determines the ankle torques that optimally provide posture equilibrium. The model also assumes that the optimal control of the system is a linear combination of the states. By using the algebraic Riccati equation, a feedback gain $\boldsymbol{K}_v$ can be determined. This gain results in a second control input torque of

$$u = -\boldsymbol{K}_v\hat{x} \tag{9}$$

A second time delay of 80 ms is included in this feedback path, to approximate the time delay involved with vestibular/visual inputs, and is implemented in the same way as the reflexive delay. The only difference between the reflex and vestibular/visual feedback loops, besides the obvious difference in the delay time, is that the white noise input into the vestibular/visual feedback loop is filtered by a low-pass filter with a corner frequency of 0.1 Hz, representing the physical plant of the vestibular organs, tending to filter out some of the higher-frequency noise. The noise matrix $\boldsymbol{N}_v$ is set to 0.04, making the variance of the vestibular/visual state error less than 1 deg for each estimated sway angle.

The system as just described accurately models quiet standing of a person on Earth. An additional variable was added to the model to account for the changes in neuromuscular characteristics following reduced gravity exposure. A variable muscle gain G is input into the plant preceding the muscle model. This scalar value represents the neuromuscular gains of the legs and is applied to the control signals in both axes before the signals reach the plant, allowing for muscular adaptation during reduced gravity stimulus. The complete model is shown in Fig. 2. The estimator-based model is used to validate the hypothesis that postural stability changes following low-gravity exposure could result from changes in muscular activation levels.

The model fails to explicitly account for the influence of vision in postural sway, since all of the experimental trials were conducted with eyes open. A future model could incorporate a visual feedback path by conducting half of the posture trials with eyes open and the other half with eyes closed, allowing visual influence to be determined and modeled.

Experimental Method

Ten healthy subjects, five men and five women, participated in the experimental study. Subjects ranged in age from 20 to 30 years, height from 1.57 to 1.95 m, and weight from 512 to 936 N. All of the subjects were in good physical condition, felt totally comfortable running at speeds over 3 m/s, and were free from any orthopedic or respiratory problems. Informed consent was obtained for all experiments; the study was approved by the Committee on the Use of Humans as Experimental Subjects; and subjects were permitted to withdraw from the study at any time and for any reason.

Acute exposure to simulated Martian gravity ($\frac{3}{8}\,g$) running served as the stimulus to elicit the heavy legs phenomenon. Reduced gravity was simulated via a suspension apparatus that incorporates a bicycle seat harness, suspension cables, springs, and an electric winch to unload five-eighths of the subject's weight (see Fig. 3). Pilot studies with three subjects were conducted in the suspension apparatus where subjects ran at 3 m/s on a treadmill at 1 and $\frac{3}{8}\,g$ and at 1 g not in the apparatus. The suspension simulator and treadmill are capable of simulating loading levels from 5 to 100% normal Earth gravity at speeds ranging from 0.5 to 4.5 m/s. No significant differences were seen in the 1 g cases for stride frequency or COP displacement; therefore, it is assumed that the results presented herein are not artifacts of

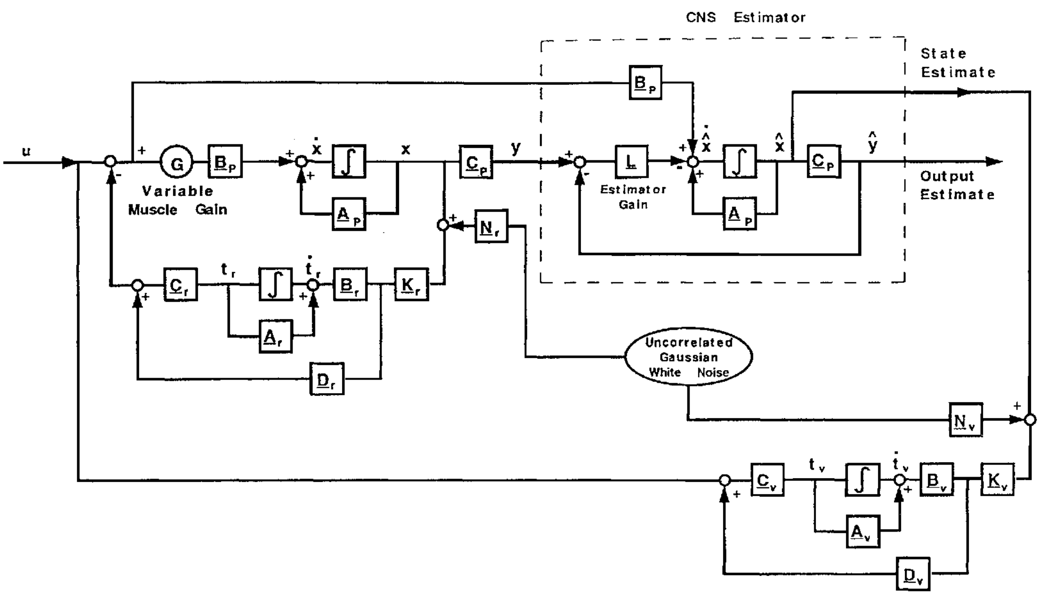

Fig. 2 Complete estimator-based state space model of posture.

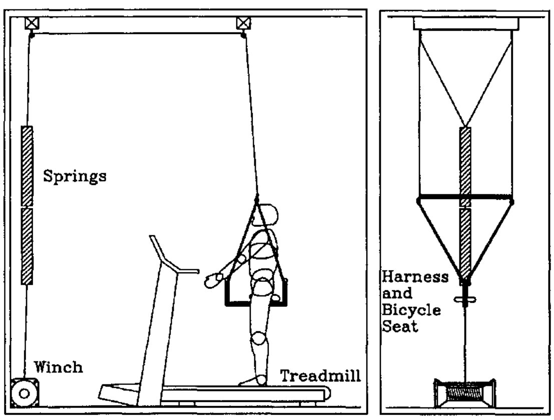

Fig. 3 Partial gravity suspension system simulator and treadmill.

the simulator per se, but of the simulated reduced gravity. While suspended at a Martian loading level, subjects ran on a treadmill at 3 m/s for 6 min. Before the reduced gravity exposure, eight (preexposure) 30-s quiet standing posture trials were recorded on a force platform. Following completion of the reduced gravity running, the subject quickly egressed from the harness and began one of three recovery-aiding exercises, no exercise, a series of five deep knee bends, or a series of three broad jumps. The subject then completed a series of six (postexposure) 30-s quiet standing posture trials. Measurements of the COP trajectory were taken while subjects stood on an Advanced Medical Technology, Inc. (Newton, Massachusetts), OR6-5 instrumented force platform with their feet a comfortable distance apart. Subjects were instructed to stand normally, with their hands at their sides while fixating on a point directly in front of them at eye level 1 m away. Force platform data were sampled at 200 Hz and consisted of forces and moments in the x, y, and z directions.

Data Analysis

The data analysis process began by discarding the first and last 5 s of each trial to eliminate the effects of unusually large sways that could have taken place early or late during the trial. Sways in the beginning of the trial might have been present if the subject, making last minute stance adjustments, was not completely stable when data collection began. In addition, since elapsed time was called out to the subject during the trial, sways could have also occurred as a result of the subject anticipating the end of the data acquisition. The average position was subtracted from the x and y (shear force direction) position to give the subject's position zero mean in each axis. The rms position of the COP was determined in the x and y axes and also as a planar (resultant) rms.

Temporal analysis is complex and assumes that quiet standing is a random process and that, although COP position cannot be predicted outright, it is possible to characterize its behavior stochastically. It is assumed that standing can be modeled as a two-dimensional random walk or as a pair of uncoupled one-dimensional random walks.[19] Over time, the mean square displacement $\langle \Delta x^2 \rangle$ of a one-dimensional random walk is related to the time interval Δt by Eq. (10):

$$\langle \Delta x^2 \rangle = 2D\Delta t \tag{10}$$

The diffusion coefficient D or the average measure of stochastic activity of the person standing increases as stochastic activity increases. This relationship can be further generalized by the nonlinear relationship

$$\langle \Delta x^2 \rangle = \Delta t^{2H} \tag{11}$$

The correlation coefficient H can be any real number between 0 and 1. The term H is somewhat more revealing than D in that H relates past trends in data to future behavior of the system. An H value of 0.5 corresponds to classical Brownian motion where past behavior is in no way related to future behavior of the system. If $H > 0.5$, the system is said to exhibit persistence, meaning that the system is likely to keep behaving in the same manner as it previously behaved. The opposite situation occurs when $H < 0.5$, or when the past and future increments of system behavior are negatively correlated (i.e., the system is more likely to change behavioral patterns), and is referred to as antipersistence.

The first step in analyzing the posture trial data in the time domain involves comparing the position of the COP at time t to the position of the COP at time $t + \Delta t$ as Δt goes from 0 to 10 s. This technique is based on Collins and De Luca's stabilogram-diffusion analysis.[19] Because of the natural variation in temporal signatures, it was necessary to average several trials. Therefore, either eight (preexposure) trials or six (postexposure) trials were averaged together. The average is then plotted with average squared distance between COP points ($\langle r^2 \rangle$) vs change in time (Δt). The resulting plot is composed of two lines with different slopes (twice the short-term diffusion coefficient D_s and twice the long-term diffusion coefficient D_l), the first with a higher slope than the second. The intersection of these lines is defined as the critical point. The diffusion coefficients are found through simple regression with the short time constant lines forced to cross through the origin and the long time constant line allowed two degrees of freedom (slope and intercept). By plotting the mean square distance vs the time interval on a log-log scale, one can calculate the values of the correlation factor H for the system through regression, allowing two degrees of freedom for both the short-term and long-term behavior.

Results and Discussion

The model data are plotted with the experimental data to facilitate direct comparison. By matching the spatial characteristics of the experimental data, the model also replicates the temporal aspects of the posture data, and through manipulation of the variable muscle gain, the postexposure changes in postural performance are duplicated. The model uses stochastic inputs yielding slight changes with every trial, much like the human subjects' data. Because of the stochastic nature of the system, only general predictions of the overall behavior can be made. A model variable is considered to match the experimental variable if the results of the model are stochastically similar to the subject data.

Changes in the spatial characteristics of the COP are shown in Fig. 4 for all four experimental test conditions as well as for four different model gains. COP displacement was recorded in both the x and y axes, and planar rms COP displacement is plotted. Interestingly, there was less sway in the mediolateral (side-to-side) than in the anteroposterior (fore-aft) direction. By providing a stable base of support, our feet keep us from swaying too far laterally. This is not true in the x axis, and as a result, the magnitude of body sway is much larger front to back. Subject data were normalized by each individual's preexposure baseline data to negate the large intersubject differences. Figure 4 also shows that the inverted pendulum estimator model produces results strikingly similar to the experimental measurements by averaging results of 20 trials performed by the model with a muscle gain of 1.0. Nine of ten subjects show significant increases in COP rms during quiet standing immediately following acute partial gravity exposure. Subject A shows a decrease in rms for all conditions following partial gravity exposure; therefore, his data are not included in the figure and are discussed later. A significant increase ($p < 0.001$) in rms COP displacement of nearly 20% is seen when subjects perform no exercise immediately following acute partial gravity exposure, and this result is replicated with a model muscle gain of 0.93. By lowering the variable muscle gain in the model, the rms increases in each axis. The COP rms increases even when subjects perform quasistatic (high force with constant rate) deep knee bends immediately following acute partial gravity, but this change is not significant. There was almost no change in the COP rms when subjects perform high-force, high-velocity broad jumps immediately following acute partial gravity exposure as compared with preexposure data. The model replicates the data using gains of 0.95 and 0.98 corresponding to knee bend and broad jump activities, respectively.

The increase in COP rms was most pronounced in the case when no postexposure exercise was performed and least evident when broad jumps were performed. From these results, it is concluded that the neuromuscular changes that occur during brief exposure to reduced gravity can be countered through exercise, and time rate of change of force is thought to be a critical variable agreeing with the results of Cavanaugh et al.,[21] who suggest that it is an important variable in reducing bone loss. Deep knee bend exercise delivering high peak forces helps to alleviate the changes brought on by low-gravity locomotion. Broad jump exercise that provides both high peak forces and high rates of change in forces is even more successful in combating the debilitating effects of partial gravity simulation. Apparently these exercises cause the body to readapt to the 1 g environment more quickly than normally occurs without exercise.

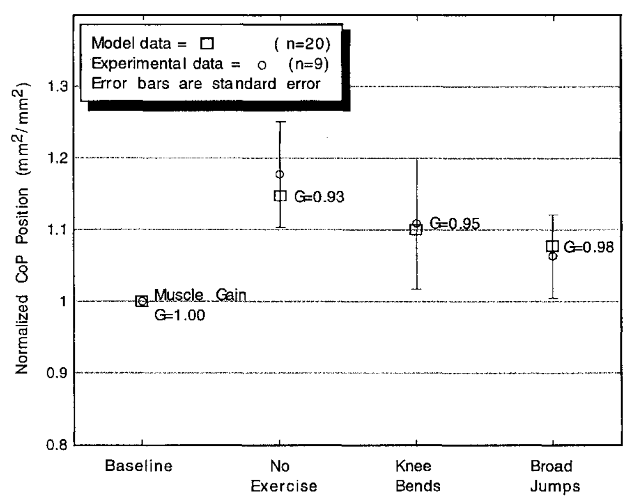

Fig. 4 Normalized COP position vs post partial gravity exposure for experimental and model data.

Recall that the time domain analysis involves comparing the COP position at time t with the position at time $t + \Delta t$ as Δt goes from 0 to 10 s. This technique is based on the stabilogram-diffusion method previously described. Figure 5a shows the general form of the total squared distance (linear sum of x and y values) between COP points vs time for subject J's experimental data. Notice the steep slope at low time intervals and a longer, more shallow slope at higher time intervals. The diffusion coefficient D is half the slope and reflects the random activity of the system within a specified interval. The critical time and critical distance are derived from the critical point (close-up detail). Although there is no change postexposure across exercise conditions as compared with preexposure, the experimental data replotted in Fig. 5b (solid lines) show that the

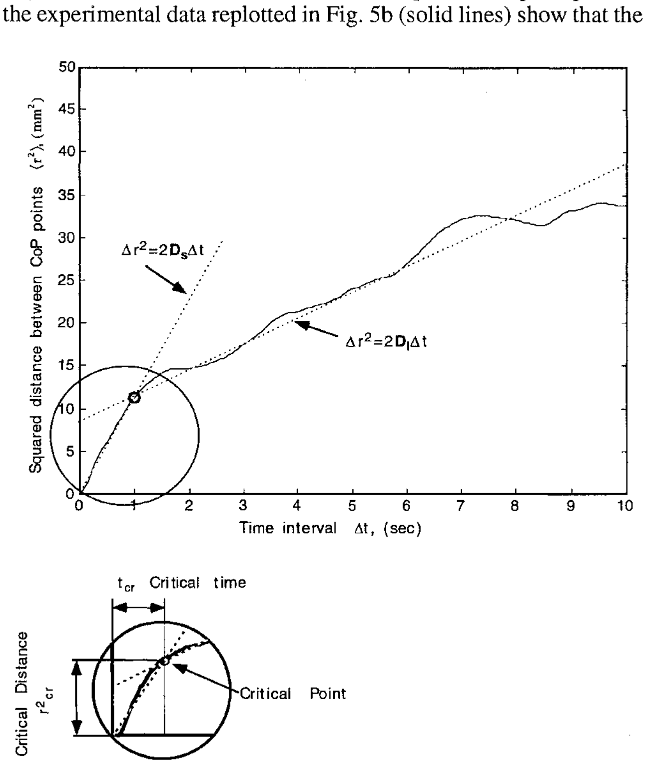

Fig. 5a Stabilogram-diffusion plot schematically showing experimental temporal data (solid) and slopes (dotted).

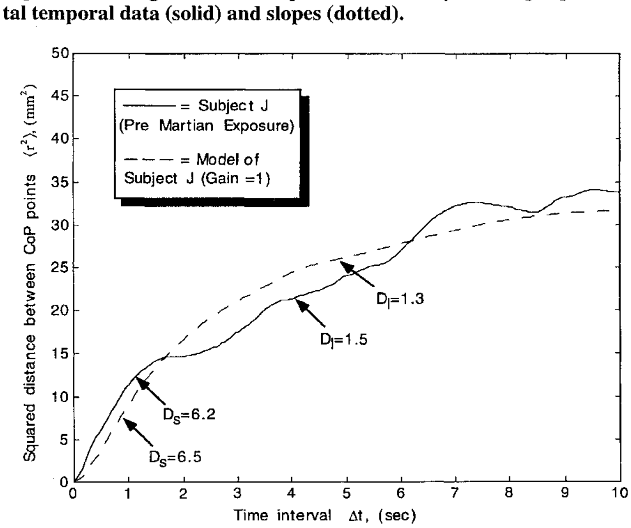

Fig. 5b Model data revealing successful replication of subject data in the preexposure condition.

short-term diffusion coefficient ($D_s = 6.2$) is significantly higher than the long-term coefficient ($D_l = 1.5$) ($p < 0.001$), indicating a higher level of stochastic activity in the short term than in the long. The model data (Fig. 5b, dotted lines), like the human subject, possess natural sway in each trial, and so 20 trials were averaged and show diffusion coefficients that are similar to those found in the experimental data ($D_s = 6.5$ and $D_l = 1.3$).

As with the diffusion coefficients, no significant change is noted in correlation coefficient H of the COP for any of the postexposure conditions. However, H_s is significantly greater than 0.5 ($p < 0.0005$), whereas H_l is significantly lower than 0.5 ($p < 0.0005$), representing persistent behavior where the COP tends to keep moving in the direction that it is currently moving and antipersistent behavior where the COP is more likely to move in the opposite direction, respectively. The short-term persistence is caused by the inertial properties of the system, because a physical system tends to move in one direction until an outside force changes that direction. The antipersistence seen in the long term is a result of the closed-loop nature of the plant. Since failure to reverse direction would result in falling over, antipersistence must be practiced. Table 1 shows the correlation coefficients for subject data compared with the variables produced by the model. The model replicates results that fall within the population of the experimental data, verifying success in capturing the important temporal characteristics of quiet standing.

The protocol followed for the posture experiment is based largely upon experiments conducted by Collins and De Luca[19]; therefore, similar results were expected. Fortunately, that is the case. In accordance with Collins and De Luca's findings, a difference is noticed between the long- and short-term temporal characteristics of human posture. The short-term behavior of the COP trajectory time trace exhibits considerably more random behavior than the long-term. Also, the short-term behavior shows a persistent trend, whereas the long term shows antipersistent trends. However, a discrepancy arises over the interpretation of results. Collins and De Luca refer to the short-term behavior as open loop and the long-term behavior as closed loop. As our model has shown, the system loop is continuously closed. Thus, the observed behavior must have an alternate explanation. The short-term persistence can be explained by the inertial characteristics of the system. As an inverted pendulum swings in any direction, its motion tends to stay in that direction until an outside force (ankle torque) changes the direction. Because of the mass of the system and, therefore, moment of inertia of the system, the change cannot be instantaneous. The combination of mass and inertial characteristics leads to persistent behavior. The long-term behavior is more a product of the loop closure than the model plant itself. Without closed-loop control, any perturbation in the states would cause the system to go unstable (i.e., the subject would fall). By closing the loop, stability is attained by reversing the direction of motion when the subject starts to fall. The reversal of motion direction is necessary to maintain stability and causes the plant to exhibit antipersistent behavior.

However, our initial model explains everything except why one subject actually underwent a decrease in rms position rather than an increase. According to the hypothesis of reduced gains in lower leg musculature for postural control, and also according to the model developed, an increase in postural sway is expected. Enhancing the model with one additional element explains the altered response of subject A. Initially, the model ignored the effects of voluntary hyperactivation of the leg muscles. In fact, the model assumes no voluntary corrective action. By adding a cognitive variable into the feedback path, the model can replicate the response elicited by subject A while continuing to properly predict performance for the other nine subjects. The subjects were instructed not to change their postural strategies during the postexposure trials. Nine of ten subjects appear to have followed these directions and did not change their postural strategy, and hence their performance was adversely affected by the decrease in neuromuscular gain. It is proposed that subject A was aware of the decreased muscular gain, and in an effort to compensate for this decrease, the subject cognitively increased his muscular activity level to enhance performance. This seems plausible since subject A was a fully informed subject and was totally aware of the hypothetical changes that would take place following reduced gravity exposure.

The model is enhanced by inserting a cognitive variable gain in the vestibular/visual feedback path, as shown in Fig. 6. Like the variable muscle gain in the plant, this cognitive gain has a very narrow band

Table 1 Comparison of correlation coefficient H for the short-term (s) and long-term (l) period where persistence is $H > 0.5$ and antipersistence is $H < 0.5$

Correlation factor, H	Baseline	Model gain = 1	No exercise	Knee bends (high force, F)	Broad jumps (high F and dF/dt)
Short term, H_s	0.71	0.73	0.55	0.51	0.51
Long term, H_l	0.25	0.23	0.27	0.23	0.26

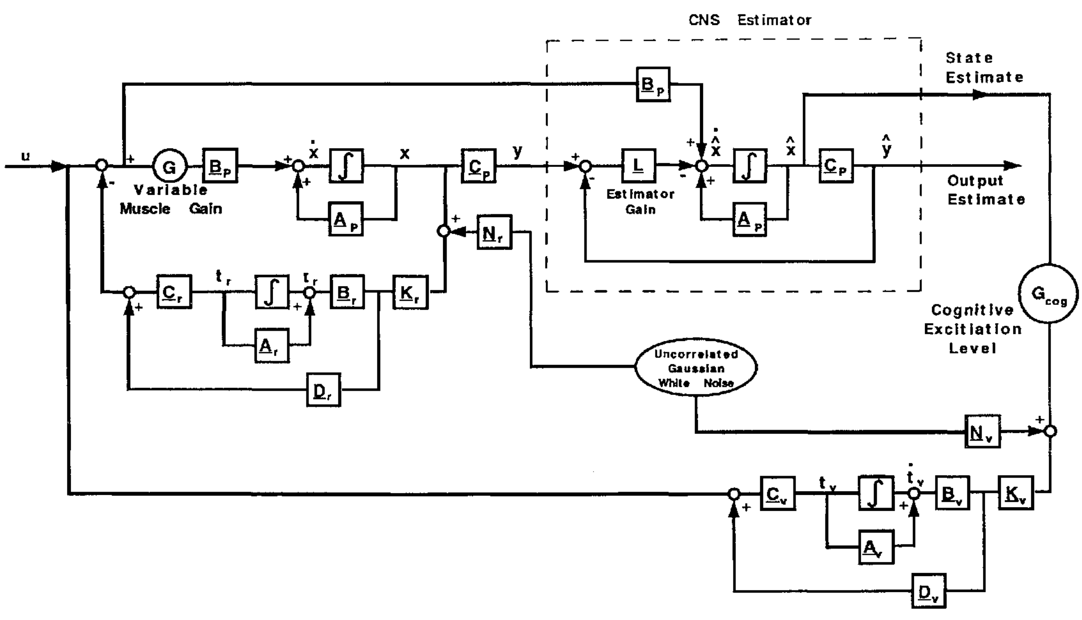

Fig. 6 Complete estimator-based state space posture model including variable cognitive excitation level.

of stability and finds support in the literature.[17,22] Despite this fact, through careful choice of gain magnitude, the inclusion of a variable cognitive activation gain in the model produced results similar to the results exhibited by subject A. The rms values of COP actually decrease in the postexposure case, even though the muscular gains were decreased.

The derived estimator-based model provides an excellent representation of human posture, capturing both the spatial and temporal qualities of COP trajectory over time. The reflex loop by itself produces a quick, jerky response yet succeeds in stabilizing the inverted pendulum plant. This modeled response might be akin to the sway oscillations noted by Paloski et al.[18] The addition of vestibular/visual cues provides a smoother response that more closely resembles the actual trajectory followed by the COP. The model could be used to enhance the experimental space flight results of Kenyon and Young.[17] Additionally, the use of a variable muscle gain within the plant produces the same result as reduced gravity locomotion, resulting in larger postural sway and higher values of rms COP displacement. The specific value of the muscle gain is not as important as the trend produced by muscular gain manipulation. By lowering the gain, the rms value significantly increases. The estimator-plant model becomes unstable, and the subject falls if the gain is lowered enough. Postural instability occurs at gains below 0.75. By raising the gain above 1.0, the system improves performance slightly, but eventually this too causes instability. In fact, the range of stable gains is between 0.75 to 2.5, and performance begins to suffer greatly even before instability ensues. A variable gain representing cognitive processes enhanced the model and accounted for the heavy legs phenomenon as well as conscious stiffening of the musculoskeletal system by a subject.

Conclusions

The estimator-based model presented in this paper captures the important aspects of human posture during quiet standing after reduced gravity exposure. The utility lies in applying control theory to quantify human performance with muscular actuators represented in state space, an inverted pendulum plant, sensory feedback pathways including Pade approximations of pure time delays using nonminimum phase zeroes and stable poles creating lag without changing the system gain, an internal estimator representing the CNS using the algebraic Riccati equation, uncorrelated white noise modeling sway uncertainty (affecting both feedback pathways), and variable gains for muscular activation and cognitive processes. The use of variable muscle gain in the model supports the hypothesis that the heavy legs phenomenon experienced after simulated reduced gravity locomotion is caused by an existing decrease in the neuromuscular gain of the lower legs from altered gravity exposure. In the case of an emergency egress, astronauts experiencing this decrement in ability may be at risk. The model replicates experimental results and offers a new approach to assess critical space flight questions of astronauts' deconditioning while in reduced gravity and their ability to stably stand upright after reduced gravity exposure.

References

[1]Greene, P. R., and McMahon, T. A., "Reflex Stiffness of Man's Anti-Gravity Muscles During Kneebends While Carrying Extra Weights," *Journal of Biomechanics*, Vol. 12, March 1979, pp. 881–891.

[2]Hogan, N., "Impedance Control: An Approach to Manipulation—Part I: Theory," *Journal of Dynamic Systems, Measurement and Control*, Vol. 107, March 1985, pp. 1–7.

[3]Hogan, N., "Impedance Control: An Approach to Manipulation—Part II: Implementation," *Journal of Dynamic Systems, Measurement and Control*, Vol. 107, March 1985, pp. 8–16.

[4]Hogan, N., "Impedance Control: An Approach to Manipulation—Part III: Applications," *Journal of Dynamic Systems, Measurement and Control*, Vol. 107, March 1985, pp. 17–24.

[5]Newman, D. J., Jackson, D. K., and Bloomberg, J., "Altered Astronaut Performance in Downward Jumping Following Space Flight-II. Mass Center Kinematics," *Experimental Brain Research* (submitted for publication).

[6]Hatze, H., "The Complete Optimization of a Human Motion," *Mathematical Biosciences*, Vol. 28, 1976, pp. 99–135.

[7]Levine, W. S., Zajac, F. E., Belzer, M. R., and Zomlefer, M. R., "Ankle Controls That Produce a Maximal Vertical Jump When Other Joints Are Locked," *IEEE Transactions on Automatic Control*, Vol. AC-28, No. 11, 1983, pp. 1008–1016.

[8]McMahon, T. A., *Muscles, Reflexes, and Locomotion*, Princeton Univ. Press, Princeton, NJ, 1984.

[9]Pandy, M. G., Anderson, F. C., and Hull, D. G., "A Parameter Optimization Approach for the Optimal Control of Large-Scale Musculoskeletal Systems," *Journal of Biomechanical Engineering*, Vol. 114, No. 4, 1992, pp. 450–460.

[10]Pyykko, I., Aalto, H., Starck, J., and Ishizaki, H., "Postural Stabilization on a Moving Platform Oscillating at High Frequencies," *Aviation Space and Environmental Medicine*, Vol. 64, No. 4, 1993, pp. 300–305.

[11]Hill, A., "The Heat of Shortening and the Dynamic Constants of the Muscle," *Proceedings of the Royal Society of London, Series B*, Vol. 126, 1951, pp. 136–195.

[12]Dietz, V., and Horstmann, G. A., "Afferent Control of Posture," *Tutorials in Motor Neuroscience*, edited by J. Requin and G. E. Stelmach, Kluwer, Dordrecht, The Netherlands, 1991, pp. 209–222.

[13]Paulus, W., Straube, A., and Brandt, T., "Visual Stabilization of Posture: Physiological Stimulus Characteristics and Clinical Aspects," *Brain*, Vol. 107, Pt. 4, 1984, pp. 1143–1163.

[14]Ring, C., Nayak, U., and Isaacs, B., "The Effect of Visual Deprivation and Proprioceptive Change on Postural Sway in Healthy Adults," *Journal of the American Geriatric Society*, Vol. 37, No. 8, 1989, pp. 745–749.

[15]Collins, J., and De Luca, C., "The Effects of Visual Input on Open-Loop and Closed-Loop Postural Control Mechanisms," *Experimental Brain Research*, Vol. 103, No. 1, 1995, pp. 151–163.

[16]Paloski, W., Reschke, M., Black, F., Doxey, D., and Harm, D., "Recovery of Postural Equilibrium Control Following Spaceflight," *Annals of the New York Academy of Sciences*, Vol. 656, May 1992, pp. 747–754.

[17]Kenyon, R., and Young, L., "M.I.T./Canadian Vestibular Experiments on the Spacelab-1 Mission: 5. Postural Responses Following Exposure to Weightlessness," *Experimental Brain Research*, Vol. 64, No. 2, 1986, pp. 335–346.

[18]Paloski, W., Bloomberg, J., Reschke, M., and Harm, D., "Spaceflight-Induced Changes in Posture and Locomotion," *Proceedings of the International Society of Biomechanics XIVth Congress* (Paris), International Society of Biomechanics, Nedlands, Australia, 1993, pp. 40, 41.

[19]Collins, J., and De Luca, C., "Open-Loop and Closed-Loop Control of Posture: A Random-Walk Analysis of Center-of-Pressure Trajectories," *Experimental Brain Research*, Vol. 95, No. 2, 1993, pp. 308–318.

[20]van den Kroonenberg, A., "Dynamic Models of Human Falls for Prediction of Hip Fracture Risk," Ph.D. Thesis, Dept. of Mechanical Engineering, Massachusetts Inst. of Technology, Cambridge, MA, 1995.

[21]Cavanaugh, P., Davis, B., and Miller, T., "A Biomechanical Perspective on Exercise Countermeasures for Long Term Spaceflight," *Aviation Space and Environmental Medicine*, Vol. 63, No. 6, 1992, pp. 482–485.

[22]Bloomberg, J. J., Peters, B. T., Smith, S. L., Huebner, W. P., and Reschke, M. F., "Locomotor Head-Trunk Coordination Strategies Following Space Flight," *Journal of Vestibular Research* (submitted for publication).